Review Article

Nanocomposites of polymer and inorganic nanoparticles for optical and magnetic applications

Shanghua Li[1]*, Meng Meng Lin[2], Muhammet S. Toprak[1], Do Kyung Kim[2,3] and Mamoun Muhammed[1]

[1]Division of Functional Materials, Royal Institute of Technology, Stockholm, Sweden; [2]Institute for Science and Technology in Medicine, Keele University, Stoke-on-Trent, UK; [3]International Research Center of Bioscience and Biotechnology, Jungwon University, Goesan-Gun Chungcheongbuk-Do, South Korea

Abstract

This article provides an up-to-date review on nanocomposites composed of inorganic nanoparticles and the polymer matrix for optical and magnetic applications. Optical or magnetic characteristics can change upon the decrease of particle sizes to very small dimensions, which are, in general, of major interest in the area of nanocomposite materials. The use of inorganic nanoparticles into the polymer matrix can provide high-performance novel materials that find applications in many industrial fields. With this respect, frequently considered features are optical properties such as light absorption (UV and color), and the extent of light scattering or, in the case of metal particles, photoluminescence, dichroism, and so on, and magnetic properties such as superparamagnetism, electromagnetic wave absorption, and electromagnetic interference shielding. A general introduction, definition, and historical development of polymer–inorganic nanocomposites as well as a comprehensive review of synthetic techniques for polymer–inorganic nanocomposites will be given. Future possibilities for the development of nanocomposites for optical and magnetic applications are also introduced. It is expected that the use of new functional inorganic nano-fillers will lead to new polymer–inorganic nanocomposites with unique combinations of material properties. By careful selection of synthetic techniques and understanding/exploiting the unique physics of the polymeric nanocomposites in such materials, novel functional polymer–inorganic nanocomposites can be designed and fabricated for new interesting applications such as *optoelectronic* and *magneto-optic* applications.

Keywords: *nano-filler*; *nano-inclusion*; *hybrid*; *effective additive*; *surface modification*; *superparamagnetism*; *UV absorption*; *in-situ polymerization*; *dichroism*

Shanghua Li received a BSc in chemistry from Tsinghua University, Beijing, China in 2003. After a Masters at the Royal Institute of Technology (KTH) in Sweden in 2004, he obtained a PhD in materials chemistry in 2008 there also. His research interests include nanostructured thermoelectrics, polymer–inorganic nanocomposites, solid oxide fuel cells, enhanced surfaces for heat transfer, and nanofluids.

Meng Meng Lin received a BSc in biotechnology at the University of Hong Kong, China, in 2004 and an MSc in biomedical nanotechnology at Newcastle University, UK, in 2005. She is currently working toward her PhD at the Institute of Science and Technology in Medicine, Keele University, UK. She was a visiting student at the Royal Institute of Technology, Sweden, in 2006. Her research interests include nanoparticles preparation, cell/nanomaterials interface, and cancer-oriented drug delivery.

Muhammet S. Toprak is a Knut and Alice Wallenberg (KAW) Research Fellow at the Royal Institute of Technology (KTH, Sweden). He graduated in chemistry education at the Middle East Technical University (METU, Turkey). After a Masters in inorganic chemistry at METU, in 2003

Significant scientific and technological interest has focused on polymer–inorganic nanocomposites (PINCs) over the last two decades. The use of inorganic nanoparticles into the polymer matrix can provide high-performance novel materials that find applications in many industrial fields. As a result of the development in nanotechnology, inorganic nanostructured materials have been designed/discovered and fabricated with important cooperative physical phenomena such as superparamagnetism, size-dependent band-gap, ferromagnetism, electron and phonon transport. Yet, they typically suffer from high manufacture expense, and the shaping and further processing of these materials is often difficult and demanding or impossible (1). Polymers, on the other hand, are flexible lightweight materials and can be produced at a low cost. They are also known to allow easy processing and can be shaped into thin films by various techniques such as dip-coating, spin-coating, film-casting, and printing. Polymers are already widely used in the optoelectronics industry and are playing important roles in various applications. Therefore, the drawbacks of using inorganic nanostructured materials can be overcome by employing a polymer matrix to embed a relatively small content of inorganic nanoparticles. The integration of inorganic nanoparticles into a polymer matrix allows both properties from inorganic nanoparticles and polymer to be combined/enhanced and thus advanced new functions can be generated to the PINCs.

The PINCs are one kind of composite materials comprising of nanometer-sized inorganic nanoparticles, typically in the range of 1–100 nm, which are uniformly dispersed in and fixed to a polymer matrix. In this way, the inorganic nanoparticles are acting like 'additives' to enhance polymer performance and thus are also termed 'nano-fillers' or 'nano-inclusions' (2, 3). Twenty years ago, the term 'nanocomposite' was not popular and 'hybrid' or 'molecular composite' were used instead (4). In that time, inorganic fillers had already been used as additives for polymers to enhance mechanical, thermal, and chemical stability. However, traditional fillers were often in micron-size and did not possess the superior properties of nanoparticles. Currently, 'hybrid' materials also refer to one kind of organic–inorganic composites that are usually made by a sol–gel method using metal alkoxides and organic molecules (5–7). Recently, among various PINCs, there is a new class of PINCs comprised of a polymer matrix with 'transparent nano-fillers' that is usually fabricated by *in-situ polymerization* for the formation of nanocomposite and sol–gel methods for the formation of nano-fillers. This class of material is also sometimes called polymer–inorganic 'hybrid/nanohybrid' (8–10).

According to Caseri (11, 12), a polymer–Au nanocomposite was probably the first reported PINC in the literature by Lüdersdorff (13). A gold salt was reduced

he obtained his PhD in materials chemistry at KTH. He was then assistant lecturer and subsequently moved to the University of California–Santa Barbara as a Postdoctoral Research Fellow receiving a prestigious award from KAW Foundation. He is now focusing on the development and use of synthetic strategies for the fabrication of nanomaterials and nanocomposites for applications in the field of energy, environment, and medicine.

Do Kyung Kim received a PhD in nanobio from the Royal Institute of Technology, Sweden in 2002. He was a Postdoctoral Fellow at the Massachusetts Institute of Technology (MIT), in 2003. He is currently a lecturer at the Institute of Science and Technology in Medicine, Keele University, UK, and a professor at the International Research Center of Bioscience and Biotechnology, Jungwon University, Korea. His research interests include target-oriented drug delivery systems, contrast agents, and quantum dots for nanomedicine.

Mamoun Muhammed received a BSc from Cairo University and a PhD from the Royal Institute of Technology in 1975. He is Chair Professor and Head of Functional Materials Division at the Royal Institute of Technology, Sweden. He has published over 200 papers, co-edited one book, and has been a guest editor for two special volumes in the *Nanostructured Materials Journal*.

in the presence of gum arabic, and subsequently a nanocomposite in the form of a purple solid was obtained by coprecipitation of gum arabic and gold in ethanol. The as-synthesized composite showed interesting optical properties such as dichroism. Before put into polymer, Au nanoparticles had already been incorporated into glass to make colored glasses that were known as gold ruby glasses. Scientists such as Neri (14) described the preparation of gold ruby glasses in the seventeenth century. In the nineteenth and early twentieth centuries, scientists such as Faraday (15), Fischer, Mie, Kirchner, and Zsigmondy (11) realized that the color of small Au particles depended on the size and distance between the particles. The size of Au nanoparticles was also experimentally determined for the first time by Siedentopf and Zsigmondy in 1903 by a light scattering method (11). After Au was first used as an inorganic nano-filler in PINC for optical applications, other metals such as Ag, Pt, Pd, Rh, Cu, and Hg were also used with natural polymers for similar optical applications (11). In 1990, the word 'nanocomposite' appeared in a paper in the polymer field for the first time when cars equipped with a

polymer–clay hybrid part were driven through towns and fields (4). Since then, polymer–clay nanocomposites, bearing superior mechanical and thermal properties than those of pristine polymers and conventional composites, became a very popular and important category of PINC. The first used polymer–clay nanocomposite was clay/nylon-6 nanocomposite for a Toyota car in order to produce timing belt covers. After that, the applications went beyond the automotive industry. For example, drink packaging was another application considering increased barrier properties of polymer–clay nanocomposites. Recently, with the rapid development of nanostructured materials that can be used as nano-fillers for PINCs, new applications of PINCs including magnetic, catalytic, electrochemical, electrical, and biomedical applications have been discovered and are described below.

Frequently employed inorganic nano-fillers include *metals* and *metal alloys* (e.g. Au, Ag, Cu, Ge, Pt, Fe, CoPt), *semiconductors* (e.g. PbS, CdS, CdSe, CdTe, ZnO), *clay minerals* (e.g. montmorillonite, vermiculite, hectorite, $CaCO_3$), *other oxides* (e.g. TiO_2, SiO_2, ferric oxide), and *carbon-based materials* (e.g. carbon nanotube (CNT), graphite, carbon nanofiber). The choice of polymer matrix is also manifold depending on the applications that can be generally divided into industrial plastics (e.g. nylon 6, nylon MXD6, polyimide, polypropylene (PP)), conducting polymers (e.g. polypyrrole, polyaniline (PANI)), and transparent polymers (e.g. polymethyl methacrylate (PMMA), polystyrene (PS)). Popular applications of PINCs include optical applications, magnetic applications, mechanical applications, catalysis, electrochemical applications, electrical and thermal applications, and biomedical applications. *Mechanical applications* (e.g. construction material) is an important application area of PINCs where industrial plastics are always chosen as the polymer matrix and clay minerals are the nano-fillers. Since smectite clay minerals – especially montmorillonite – are composed of several layers of silicates, this kind of PINCs is also called 'polymer-layered silicate nanocomposites' and the application of this kind of PINCs is called mechanical 'reinforcement.' In 2006, Okada and Usuki published a nice review on the 20-year development of polymer–clay nanocomposites (4). Recently, with the explosion of CNTs in the material research field, carbon-based materials including multi-walled CNTs, single-walled CNTs, and carbon nanofibers are used instead of clay minerals for the same applications (16). *Catalytic* and *electrochemical applications*, such as sensors, are other applications of PINCs where metals including Ge (17), Cu, Pt (18), and oxides including SiO_2, TiO_2 (19), are selected as inorganic nano-fillers. Very recently, PINCs are also used in *electrical and thermal applications*, where nano-fillers such as CNTs and carbon nanofibers are used to enhance the electrical/thermal conductivity of the conductive polymer matrix (20, 21). While Au and iron oxide nanoparticles were frequently used in *biomedical applications* (22, 23), their polymeric nanocomposites have also recently been used as an intelligent therapeutic system (24) and bioimaging agents (25). Optical and magnetic applications are two of most important application aspects of PINCs and therefore will be focused in this review. For *optical applications* of PINCs, inorganic nanoparticles of metals such as Au or Ag and semiconductors such as TiO_2, ZnO, or PbS are commonly used as 'optically effective additives' (11), while transparent polymers such as PMMA are used as polymer matrix. For *magnetic applications*, metals and metal alloys such as Fe (26, 27) or CoPt (28), oxides such as ferric oxide (29, 30), and ferrite (31) are always used as inorganic nano-fillers. Before the detailed description of these two applications of PINCs, a comprehensive review of synthetic techniques of PINCs will be introduced.

Synthetic techniques

The mixing of polymers and nanoparticles is opening pathways for engineering flexible composites that exhibit advantageous magnetic, electrical, optical, or mechanical properties. As part of this renewed interest in nanocomposites, researchers began seeking new strategies to engineer materials that combine the desirable properties of nanoparticles and polymers for the formation of PINCs. The research revealed a number of key challenges in producing PINCs with the desired behavior. The greatest hindrance to the large-scale production and commercialization of PINCs is the absence of cost-effective methods for controlling the dispersion of the nanoparticles in polymeric hosts. The nanoscale particles typically aggregate, which cancels out any benefits associated with the dimension (32). The particles must be integrated in a way leading to isolated, well-dispersed primary nanoparticles inside the matrix. There is a need for establishing processing techniques that are effective on the nanoscale yet are applicable to macroscopic processing. Synthetic strategies for PINCs with a high homogeneity are, therefore, really a challenge. There have been several attempts for the synthesis of PINCs that can be classified under two major categories: as physical and chemical methods. Physical methods include solvent processing; melt-processing, polymer melt intercalation whereas chemical methods are *in-situ* processes (33) as will be detailed in the following sections.

Smaller particle size allows a much more homogeneous distribution of a PINC material and leads to a drastic increase of the polymer–nanoparticle interfacial area due to the high specific surface area of nanoparticles. This may induce aggregation of the nanoparticles to energetically stabilize PINCs, thus lowering the homogeneity of particle distribution. In order to minimize interface energies between particles and polymer matrix, several

surface modification/functionalization and stabilization techniques have been developed that are mainly used in chemical methods (1).

Physical methods

Physical preparation methods for PINCs are based on liquid particle dispersions, but differ in the type of the continuous phase. In melt processing, particles are dispersed into a polymer melt and then PINCs are obtained by extrusion. Casting methods use a polymer solution as a dispersant and solvent evaporation yields the PINC material (1). Fig. 1 gives an overview of melt processing and film casting approaches.

Melt compounding has been used for a wide range of materials such as clays, oxides, and carbon nanotubes. An important strength of this route is the large quantity of material that can be produced by extrusion, since most polymer blends are commercially produced in this way due to the ease and economic viability of the process. Furthermore, well-established fiber processing technology can be successfully used for processing nanocomposite fibers (34). The PP–organoclay nanocomposite fibers were obtained by melt spinning a mixture of organophilic surface modified clays and melted PP (35). Polylactide-organically modified layered silicate nanocomposites were reported that were prepared via melt extrusion of polylactide and surface modified clay-montmorillonite (36). The PP/silica nanoparticle nanocomposite filaments were prepared by direct mixing of components and melt compounding using a twin-screw extruder prior to spinning (34). Surface treated ZnO nanoparticles were also dispersed in PP via extrusion (37).

Film casting is another approach for the preparation of PINCs, in which hydrophobic nanoparticles are dissolved in a polymer solution, which is then cast or coated on substrates forming composite sheets or films upon evaporation of the solvent. Due to its simplicity, the film casting method is widely used and nanocomposite thin films are typically prepared by spin coating of the nanoparticle-polymer solution. The solvent evaporation takes place during the coating process, or by subsequent treatment in an oven, which results in the formation of homogenous films. For the solution casting, the polymer synthesis step can be separated from the particle generation and the nanocomposite processing (38). Thick polymer sheets of ZnO/PS nanocomposites were casted from a solution in N,N-dimethylacetamide followed by hot pressing to remove solvent residues in order to obtain homogenous nanocomposites (39). Thick monomer-SiO_2 nanoparticle films containing a photoinitiator were also prepared by spin coating, which were then exposed to UV-irradiation to initiate the polymerizations process to make integrated optics devices (40).

Intercalated structures are formed when a single or more extended polymer chain is intercalated between the clay layers. A scheme describing the possible interactions of polymers with layered inorganic structures is presented in Fig. 2. The result is a well-ordered multilayer structure of alternating polymeric and inorganic layers (41). Work by Giannelis and coworkers revealed that intercalation of polymer chains into the galleries of an organoclay can occur spontaneously on heating a mixture of polymer and silicate clay powder above the polymer glass transition or melt temperature (42, 43). Once sufficient polymer mobility is achieved, chains diffuse into the host silicate clay galleries, thereby producing an expanded polymer-silicate structure. Giannelis et al. also reported on the modeling of polymer melt intercalation in organically modified layered silicates (OLS) (44). From the theoretical model, the outcome of hybrid formation via polymer melt intercalation was found to depend on energetic factors that may be determined from the surface energies of the polymer and OLS. A general guideline for the production of a road map was established for selecting potentially compatible polymer–OLS systems. It was suggested that the interlayer structure of the OLS should be optimized to maximize the configurational freedom of the functionalizing chains upon layer separation and to maximize potential interaction sites at the interlayer surface (44).

Chemical methods

Direct mixing and melt processing of particles with polymers often lead gradients of the incorporated fillers in the matrix that leads to turbidity/translucency of composite materials because of the agglomeration of the nanoparticles. *In-situ polymerization* and *in-situ nanoparticle formation* methods have been developed to overcome these problems.
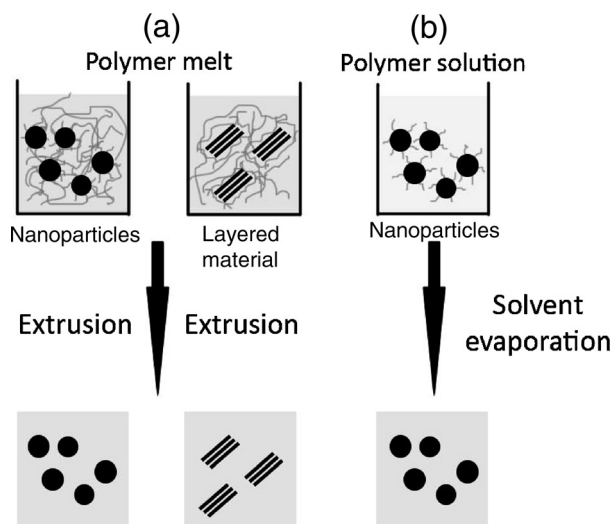

Fig. 1. Preparation methods for nanocomposites: (a) melt compounding, (b) film casting.

Polymer intercalated
between the galleries

Layered inorganic material

Completely exfoliated
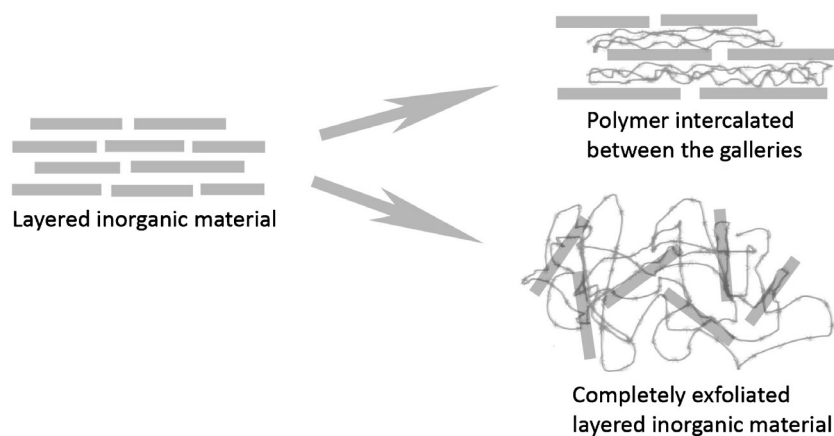layered inorganic material

Fig. 2. Schematic description of interactions between polymers and layered inorganic materials for the formation of PINCs. (Adapted from Ref. (58).)

In-situ polymerization

The procedure of *in-situ polymerization* involves dispersing the inorganic nanoparticles directly in the monomer solution prior to a polymerization process. Inorganic particles tend to phase separate and sediment pretty quickly from the organic polymer. In order to make sure a good link/interaction at the interface is obtained, specific groups have to be linked onto their surface to stabilize nanoparticle dispersions (1).

Emulsion polymerization is a common route for the synthesis of polymers. This route was utilized for the fabrication of PINCs intercalated with PMMA by an emulsion polymerization of methyl methacrylate (MMA) in the presence of Na^+-montmorillonite, without employing any modification of the monomer to impart active sites or without the addition of any coupling agents (45). The PS/clay nanocomposites were synthesized by the emulsion polymerization of styrene in the presence of sodium ion-exchanged montmorillonite, demonstrating that the strongly hydrophobic PS was intercalated into the hydrophilic silicate layers (46).

In solution chemical synthesis of nanoparticles, a careful design of experimental conditions is vital to obtain well-dispersed particles with a narrow size distribution. For this purpose several synthetic schemes have been utilized, the most effective being the formation of nanoparticles in the oil phase in the presence of amphiphilic molecules (47–50). Amphiphilic molecules, or so-called surfactants, such as long-chain carboxylic acids, amines, thiols, or alcohols can be chemisorbed on a nanoparticle surface and builds a hydrophobic interface that lowers the specific surface free energy of the inorganic particles and thus avoid nanoparticle agglomeration. Although the surfactant molecules do not directly participate in the polymerization process, they assure a good dispersion of the nanoparticles in monomers thus embedding the nanoparticles in the growing polymer during the polymerization (12, 51).

Surface-modified particles can be isolated easily from the media they are prepared in. For instance, one of the most intensively studied nanoparticle systems of iron oxide has been widely synthesized in the presence of oleic acid or oleyl amine groups that work both for confinement of particles, avoiding their uncontrolled growth and provide a very high dispersability to these nanoparticles in hydrophobic media (52). Besides oxide nanoparticles, metallic and semiconducting nanoparticles as gold, silver, and CdS and CdSe surrounded by a layer of organic thiols or carboxylic acids, where the functional thiol/carboxyl groups are attached to the particle surfaces are also reported (47–50). The synthesis process is very versatile and has also been used for the synthesis of other transition metal oxides as well as several semiconductors (50).

Oleic acid-capped Fe-oxide nanoparticles were synthesized and used for the fabrication of PMMA/Fe-oxide PINCs by *in-situ polymerization*. The presence of the oleic acid on the nanoparticle surface increased the compatibility of the inorganic particles with the polymeric matrix and yielded bulk homogeneous and highly transparent PMMA/Fe-oxide PINCs (53). Magnetic vinyl ester resin nanocomposites containing iron oxide (Fe_2O_3) nanoparticles functionalized with a bifunctional coupling agent methacryloxypropyl-trimethoxysilane was also reported. It was observed that particle functionalization favored the nanocomposite fabrication with a lower curing temperature as compared to the as-received nanoparticle filled vinyl ester resin nanocomposites (54). Calcium carbonate nanoparticles covered by acrylic and stearic acid was successfully utilized for *in-situ polymerization* with MMA. The presence of the acrylic and stearic acid on the nanoparticle surface increased the compatibility of the inorganic particles with the polymeric matrix and yielded bulk composite nanomaterials (55, 56). Silica nanoparticles coated with -3-(trimethoxysilyl)propyl self-assembled in films of methyl acrylate, MMA, and a

mixture of MMA and 2-hydroxyethyl methacrylate, which upon photopolymerization produced PINC in which the ordering of the particles is maintained (57).

The nanoparticle surface can be modified with polymerizable groups. Surface initiated polymerization (grafting from) and tethering (grafting-to) techniques are also proven to be very useful for homogenous PINCs synthesis (23, 58). A scheme describing these two approaches is presented in Fig. 3. The required functionalities can be embedded in the design of the polymer chain that will bind to, or strongly interact with, the nanoparticle surface. By reaction of these anchoring groups with functional sites at the nanoparticle surface, the polymer can be grafted onto the inorganic particle. The polymer can also be grafted from the nanoparticle surface by adsorption or covalent linkage of monomers at the surface and subsequent growth from the surface (12, 58).

An example of the grafting-to process is the PINC formation by anchored polymer coatings on alumina. Carboxylic acids are generally strongly adsorbed on oxide surfaces and in this work a polymerizable group of maleic acid adsorbed on alumina was used to copolymerize with 1-alkenes to form a monolayer of polymer that was tightly anchored on the alumina surface (59). The grafting-to method has been used to synthesize bulk ZnS-polymer PINCs by using N,N-dimethylacrylamide as a coordinating monomer for polymerization with styrene and divinylbenzene as co-monomers (60). The ZnO was also embedded in poly(butanediolmonoacrylate; PBDMA) by in-situ polymerization of the monomer dispersion with BDMA as stabilizing ligand (61).

A surface-initiated atom transfer radical polymerization (ATRP) is one of the most robust and versatile approaches for the synthesis of polymer films, due to its ease of controlling the thickness, the surface density, and the composition of grafted polymer films. Yang et al. reported on the fabrication of cross-linked PINC thin films through the combined use of the surface-initiated ATRP and gas–solid reaction (62). Lead dimethacrylate (LDMA) polymer films were grown directly from the substrates by covalent bonds with surface silanol groups. After cross-linking, PbS nanoparticles were generated

in-situ by exposing the PLDMA films to H_2S gas at room temperature.

PINCs can also be produced with grafting from techniques by functionalization of nanoparticle surfaces with initiating groups, starting the polymerization reaction from the nanoparticle surface. Different kinds of functionalization can lead to anionic, cationic, or free radical polymerization (51). This kind of surface modification is of particular importance in the area of polymer clay nanocomposites. Since the highly polar, ionic surface of clay minerals is not compatible with most polymers, such as PS, polyethylene or PP, the clay surfaces have to be modified with organic molecules in order to adapt the chemical nature of the polymer matrix, which leads to an improvement of the dispersability of the clay in the polymer matrix. An example for in-situ polymerization is in the presence of clay materials in which the initiator is linked to the surface via ionic interactions. The formation of the polymer in between the silicate layers causes delamination of the layered silicate (33). Qutubuddin and Fu reported on the synthesis of exfoliated PS–clay nanocomposites in which organophilic exfoliated montmorillonite was prepared by cation exchange with polymerizable surfactant vinylbenzyldimethyldodecyl ammonium chloride (63).

Cationic initiators are known to form strong ionic interactions with negatively charged surfaces, as found on many oxide particles since most of the oxide particles have a wide range of pH values where they exhibit a net negative surface charge. Butyl butacrylate was grafted from TiO_2 particle surfaces by using 2,29-azobis(2-amidinopropane) dihydrochloride (AIBA) as an initiator for in-situ polymerization (64).

Layer by layer (LbL) deposition of nanoparticles and polymers can also be utilized for the formation of highly homogeneous thin PINC films. An interesting example is the formation of ultrastrong and stiff layered nanocomposites by sequentially coating a surface with nanometer thick layers of poly(vinyl alcohol; PVA) and negatively charged clay montmorillonite by immersing a glass substrate in dilute solutions of components. Resulting layers were then treated with glutaraldehyde
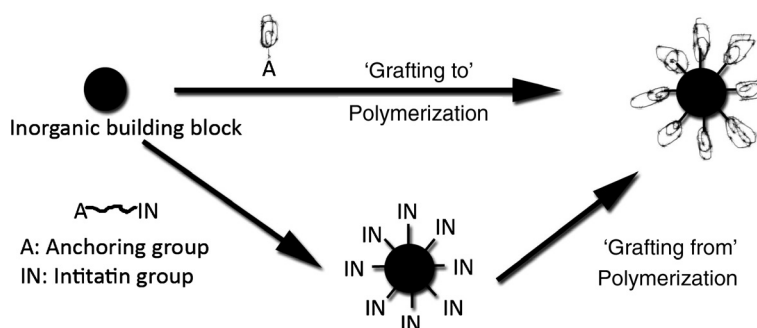

Fig. 3. Schematic description of grafting-to and grafting-from approaches for the synthesis of PINCs. (Adapted from Ref. (58).)

to cross-link –OH groups and the clay surface (65). PINCs consisting of PVA and an aqueous dispersion of colloidal silica have been prepared by the LbL technique taking advantage of the hydrogen bond formation among themselves and involving the hydroxyl group present in both the moieties, thus eliminating the need for a coupling agent (66).

Electron irradiation was also reported to be an effective and attractive method to modify the surfaces of inorganic materials and prepare PINCs. The electron irradiation technique was successfully employed to prepare PINCs of anatase and rutile TiO_2 as well as γ-Al_2O_3 nanoparticles with PMMA, where it was suggested that the active species initiating grafting polymerization may form on the nanoparticle surface by electron irradiation (67). In another report, silica and calcium carbonate nanoparticles were irradiated by ^{60}CO γ-ray in the presence of various monomers including styrene, MMA, butyl acrylate, methyl acrylic acid, and vinyl acetate as grafting monomers. Subsequently, these surface grafted primary nanoparticles were collected and mixed with melted PP for the formation of PINCs (68).

There have also been theoretical modeling attempts to describe and control the interactions between the nanoparticles and various polymer matrices during the formation of PINCs. Balazs and coworkers reported on the calculation of phase diagrams for nanocomposites to determine the equilibrium properties of polymer/clay mixtures, where both functionalized and non-functionalized clays were used (69). They suggested that the technique proposed in their work could be applied to describe the equilibrium phase behavior of other model nanocomposite or polymer/colloid systems and that the resulting phase diagrams could also be used as guidelines for the development of new composites with thermodynamically stable morphologies.

In-situ particle formation

Chemical methods based on the *in-situ* sol–gel polymerization method allows single-step synthesis of PINCs in the presence of polymer or monomer (9). This method makes it possible to manipulate the organic/inorganic interfacial interactions at various molecular and nanometer length scales, resulting in homogeneous PINC structures and thus overcoming the problem of nanoparticle agglomeration (5, 70, 71).

A simple method for the synthesis of PINCs is through the hydrolysis or reduction of metal salts in the presence of a polymer (58). For instance, composite of PANI with a ferromagnetic feature was synthesized by impregnating the polymer with iron salts followed by a treatment with alkali solution to form iron oxide nanoparticles in the polymer matrix (72).

Sol–gel processing of inorganic oxide nanoparticles either in the presence of a preformed polymer or in parallel with the formation of the organic polymer is also proven to be an effective method for the fabrication of PINCs. The process of nanoparticle formation proceeds via hydrolysis and condensation of the organometallic precursor and has been studied extensively (71). Sol–gel hydrolysis and condensation of a precursor such as tetraethoxysilane (TEOS), tetrabutyl titanate, aluminum iso-propoxide were carried out starting from a preformed functional organic polymer such as polyvinyl acetate, PMMA, polyvinyl alcohol, and several other polymers for the formation of PINCs (73–79).

Li et al. demonstrated a technique for the synthesis of transparent PMMA–ZnO PINCs. Linking inorganic and organic phases is achieved using MEA as a coupling agent between ZnO QD complexes and non-polar polymer molecules (10). In the same manner, organic–inorganic hybrid materials are simultaneously synthesized in MMA via free-radical polymerization, which permits covalent bonding with ZnO complexes. The hydroxyl groups in MEA functionalize both polymer molecule moieties and surfaces of inorganic fillers, and have the ability to form further cross-links between the immiscible surfaces and covalent bonding.

Production of thin films of photosensitive hybrid organic–inorganic glass on silicon was reported using the solution sol–gel method (40). Preformed ZrO_2 nanoparticles, via hydrolysis and condensation of organometallic precursors, were dispersed in a photopolymerizable silicate monomer matrix containing a photoinitiator, methacryloxy-propyltrimethoxysilane (MAPTMS), and methacrylic acid. Controlled hydrolysis of the MAPTMS resulted in highly homogenous PINC films.

Microemulsions are thermodynamically stable, isotropic liquid mixtures of oil (o), water (w), and surfactant, in which one of the liquids is dispersed in the other; based on their respective distribution there are two categories as normal (oil in water o/w) and inverse/reverse (water in oil w/o) microemulsions (80). Several inorganic nanoparticle systems have been synthesized via an inverse microemulsion process (80, 81). Two or more separate microemulsions can be mixed together for the particle formation via an intermicellar exchange of the reactants. A new way of producing PINCs in a single-step synthesis is the use of a microemulsion system in which the monomer is used as an oil phase, forming a completely polymerizable matrix (82).

Polyaniline/V_2O_5 core–shell nanocomposites have been successfully prepared using hexadecyl trimethyl ammonium bromide (CTAB) microemulsion (83). PINCs consisting of PMMA and SiO_2 have been synthesized using a reverse microemulsion process containing water-nonionic surfactant and methyl methacrylate (MMA) monomer as the oil phase. The SiO_2 nanoparticles formed via hydrolysis and condensation of an alkoxide precursor within nanosized microemulsion droplets followed by the polymerization of the microemulsion (84). Another

example is CdS-polyacrylamide nanocomposites prepared by γ-irradiation in w/o microemulsion. An aqueous solution containing the precursor materials for CdS and acrylamide monomers was slowly added to an oil phase containing emulsifiers until a transparent microemulsion was formed. Subsequent γ-irradiation of this emulsion resulted in a CdS–Poly acrylamide nanocomposite (85).

Optical properties and applications of PINCS

Optical properties and applications of PINCs were probably the first known functions of PINCs starting from the ancient ages and have attracted attention for centuries. Inorganic nanoparticles, especially metals and semiconductors, have received increasing attention as 'transparent nano-fillers' for the PINCs during the past two decades. PINCs for optical applications take advantage of the optical properties of materials that are hard to grow in single-crystal form or that require protection from the environment and give them the ease of processing afforded many polymers. In addition, the inorganic nanoparticles can be used to achieve specific optical properties, and the polymer matrix is used just to hold the particles together and provide processability. In this chapter, the ability of inorganic nanoparticles to serve as optically effective additives for PINCs will be exploited. Application examples of *light absorption including UV and color* (*visible light absorption*), *photoluminescence* (PL), *extreme refractive index* (RI), and *dichroism* will be presented by selection of related results from other groups as well as our own research.

Size of the inorganic nanoparticles as nano-fillers is an important factor that affects many optical properties and applications of the PINCs. For example, the PL of polymer–semiconductor quantum dots (QDs) nanocomposites is dependent on the size of QDs; the color and RI of polymer–metal nanocomposites are also dependent on the size of metal particles. In general, the major requirement of inorganic nanoparticles to be used as optically effective additives for transparent polymers is a small size (<40 nm). Rayleigh's Law can be used to estimate the intensity loss of light passing through a composite by scattering, as shown in Equation 1:

$$\frac{I}{I_0} = e^{-\left[\frac{3\varnothing_p x r^3}{4\lambda^4}\left(\frac{n_p}{n_m}-1\right)\right]}, \tag{1}$$

where I is the intensity of the transmitted and I_0 is the incident light, $\varnothing_p$ is the volume fraction of the particles, x is the optical path length, r is the radius of the spherical particles, λ is the wavelength of light, n_p is the RI of the particles, and n_m is the RI of the matrix. It can be clearly seen from Equation 1 that the light loss by scattering steeply increases with particle size. Normally, 40 nm is an up-limit for nanoparticle diameters to avoid intensity loss

of transmitted light due to Rayleigh scattering (1). The transparency/opacity is also dependent on the difference of RI between nanoparticles and the polymer matrix, and dispersion/agglomeration of nanoparticles into the polymer matrix. When the RI of nanoparticles and the polymer matrix is close, transparency can also be achieved with bigger nanoparticles. Agglomeration of nanoparticles will cause an increase of opacity. The arrangement of nanoparticles into the polymer matrix is another important factor that affects optical properties of PINCs. Random distribution of individually dispersed nanoparticles favors optical transparency, PL, and UV absorption; ordered nanoparticles can introduce iridescence; while uniaxially oriented nanoparticles can cause dichroism (12).

Light absorption

UV absorption

With changes in atmospheric composition and the thinning of the ozone layer during the past decades, there has been a profound increase in UV radiation dosage (86). Consequently, a great deal of recent research has focused on the development of photo-protective materials, especially nanocomposites (87, 88). For this purpose, organic UV-absorbing pigments are widely used as additives to polymers to prepare UV-protective coatings. However, nanocomposites comprised of polymer and organic UV-absorbers generally suffer from low long-term stability. Inorganic UV-absorbers, on the other hand, have high photostability and are therefore of great interest as additives to polymers. A high transparency in the visible range and a steep absorption in the near UV range (λ <400 nm) are required for most applications on UV absorption. Most promising inorganic materials are nanosized ZnO and TiO_2, which have bulk band-gap energies of around 3 eV (1).

A number of studies have recently reported on the preparation of PINCs comprised of polymer and inorganic UV-absorbers (ZnO and TiO_2) by directly incorporating ZnO fillers into a polymer matrix, mainly by physical methods (89–93). Chemical methods, based on *in-situ polymerization*, were also employed to prepare PINCs for UV absorption (8, 9, 94) and are found easier to achieve a homogeneous dispersion of nanoparticles in the polymer matrix. Recently, PMMA–TiO_2 hybrid materials have been reported by Zhang et al. (8) and transparent thin films of PMMA–TiO_2 nanohybrids (9) and PMMA-ZnO nanohybrids (94) have been proposed. In all these works, inorganic nano-fillers (ZnO or TiO_2) were always synthesized first, and then either mixed directly with a melt/dissolved polymer or dispersed into the monomer followed by polymerization. To have effective UV absorption, typical ZnO/TiO_2 content of

1–35 wt% was used. The transparency can only be kept in the form of films (μm scale thick) but difficult in bulk form (mm/cm scale thick), as the increased thickness results in opaqueness/translucence.

As detailed in the subsection: *In-situ particle formation*, we have developed a new synthetic strategy for PINCs, *in-situ sol–gel polymerization*, which allows a simultaneous formation of inorganic ZnO as well as the polymer (10). The ZnO formed by a sol–gel process had a very small size in quantum range (below 10 nm) and was well-dispersed in the polymer matrix. As shown in Fig. 4, the as-synthesized PMMA-ZnO nanocomposites had a very effective UV-blocking effect even with a ZnO content as low as 0.017 wt%, while retaining high transparence in the visible range even in bulk size (1 cm thick). Faubl and Quinn (95) reported the amount of UV radiation transmitted by commercially available UV-blocking con-tact lenses and demonstrated that the thickness of the contact lens is strongly related to the efficacy of UV transmission. The transmission in the range from 290 to 340 nm is approximately zero, indicating that the PMMA-ZnO nanocomposites have a much higher shield-ing efficacy than commercially available UV-blocking contact lenses. Although the as-synthesized nanocompo-sites contain ZnO filler at a concentration about 100 times smaller than poly(styrene butylacrylate) latex-ZnO nanocomposites (7 wt% ZnO) reported by Xiong et al. (91), a stronger UV absorption and a larger blue shift are observed. It is known that for small size nanoparticles (below 10 nm), quantum confinement increases the band-gap energy and a blue shift of the absorption edge compared to the bulk material can be observed. Our studie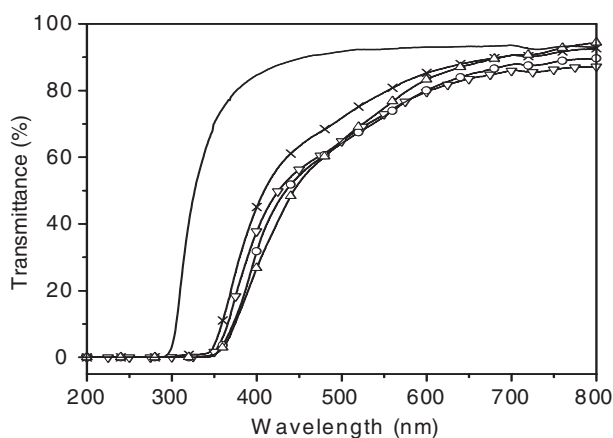s substantiated that with extremely homogenous distribution of UV-absorbers, strong UV-blocking/high UV absorption efficiency can be achieved even with a very low content of quantum-sized UV-absorbers in the polymer matrix. The thermal stability of the polymer was also enhanced by incorporating the inorganic UV-absorbers.

The particle size of ZnO QDs can be deduced from the effective mass model for spherical shapes with a coulomb interaction term (96, 97).

$$E^* \cong E_g^{\text{bulk}} + \frac{\hbar^2\pi^2}{2er^2}\left(\frac{1}{m_e m_0} + \frac{1}{m_h m_0}\right) - \frac{1.8e}{4\pi\varepsilon\varepsilon_0 r}, \qquad (2)$$

where E^* is the band-gap, E_g is the bulk band-gap, $\hbar$ is the Planck's constant divided by 2π, r is the particle radius, m_e is the effective mass of electrons, m_h is the effective mass of the holes, m_0 is the free electron mass, e is the charge on an electron, ε_0 is the permittivity of free space, and ε is the relative permittivity. Since the effective mass of electrons and holes in ZnO QDs is comparatively minute ($m_e = 0.24$, $m_h = 0.45$), the band-gap enlargements can only be observed when particles are in the quantum regime (less than 8 nm) (98). However, Equation 2 is qualitative and used only to prove the particle size is in the quantum range. It does not give a quantitative estimate of the particle size. The method proposed by Meulenkamp (99), Equation 3, based on an experimental relationship between the average diameter (D) and the absorption shoulder ($\lambda_{1/2}$) of the ZnO QDs colloids, can be used to calculate the particle size:

$$1,240/\lambda_{1/2} = 3.301 + 294.07/D^2 + 1.09/D, \qquad (3)$$

where $\lambda_{1/2}$ is the wavelength at which the absorption is 50% of the excitonic peak or shoulder and D is the particle diameter ($\lambda_{1/2}$ in nm, diameter in Å).

Color (visible light absorption)

As mentioned above, in the nineteenth and early twen-tieth centuries, it was already discovered that the color of small metallic particles depended on the size and distance between the particles (11). This can be utilized to make PINCs with a different color just by varying the size of inorganic nano-fillers. For example, Heffels et al. (100) observed in transmission that PVA–Au nanocomposites appeared pink when a particle diameter of Au is 16 nm, purple when 43 nm, and blue when 79 nm. Kirchner and Zsigmondy discovered that the color of PINCs can depend not only on the size of metallic particles but also on the distance between the particles (11). This is based on the observation that nanocomposites of gelatin and silver or gold nanoparticles changed their color upon swelling with water. Later, Maxwell Garnett (101, 102) demonstrated it with theoretical analysis. The colors of the PINCs composed of polymer and metallic nanoparticles can be retained over extended periods

Fig. 4. UV-VIS spectra of PMMA-ZnO nanocomposites as-synthesized by *in-situ sol–gel polymerization* (ZnO content: —, 0 wt%; X, 0.017 wt%; ▽, 0.026 wt%; △, 0.040 wt%; ○, 0.050 wt%, the thickness of the all the samples is 1 cm). (Adapted from Ref. (10). Reproduced with permission from Wiley-VCH Verlag GmbH & Co. KGaA.)

(11), which is advantageous when using PINCs for color applications.

Photoluminescence

High-efficient PL devices with μm-sized features are of great interest for photonic applications. Analogous to systems such as dye-doped polymers, PL semiconductor–polymer nanocomposites are also attractive as PL polymeric materials, since various semiconductor nanocrystals show unique tunable light emission properties arising from quantum size effects. Semiconductor nanocrystals, such as QDs (II–VI and III–V), can cover a large range of light emission spectra (from 400 to 1,400 nm). Compared to the organic dyes (e.g. Rhodamine 6G), QDs are 20 times brighter, 100 times more stable against photobleaching, and one-third as wide in emission linewidth (103). Due to these unique properties of semiconductor nanocrystals and good processability of their dispersions in polymer or monomers, the integration of PL nanoparticles into polymers offers a new range of promising applications in lighting and display devices.

Studies on PL PINCs started recently from the early 2000s. Lee et al. (104) and Erskine et al. (105) embedded CdSe nanocrystals in poly(lauryl methacrylate) and PS matrices, respectively. Fig. 5 shows the color fluorescence image of QD-poly(lauryl methacrylate) composite rods under a UV lamp (104). The QDs used in Fig. 5 were ZnS-overcoated CdSe with a core radii of 10, 23, and
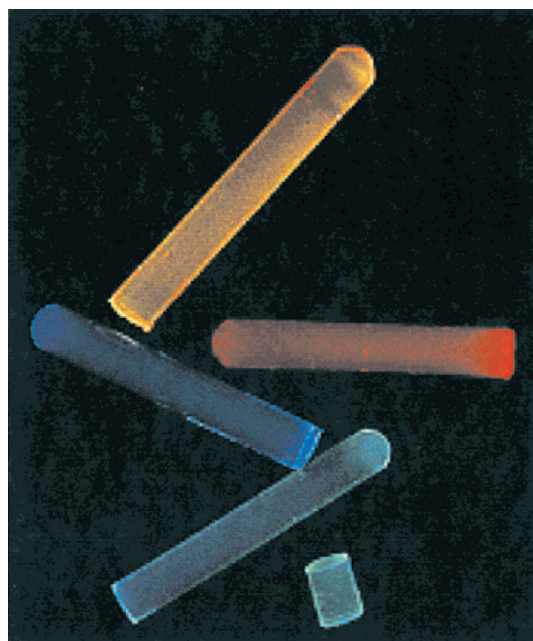

Fig. 5. Color fluorescence image of QD-poly(lauryl methacrylate) composite rods excited by a UV Hg-lamp ($\lambda_{em} = 365$ nm). (Adapted from Ref. (104). Reproduced with permission from Wiley-VCH Verlag GmbH & Co. KGaA.)

28 Å, showing nearly pure color emissions (104). Farmer and Patten (106) reported synthesis of PL films comprised of core-shell CdS/SiO$_2$ as inorganic nano-fillers and PMMA as the polymer matrix. Zhang et al. (107) incorporated fluorescent CdTe nanocrystals into PS and PMMA. In 2008, Sun et al. (108) and Ventura and Gu (109) demonstrated 3-D photonic crystals based on embedding polymer with CdS and PbSe QDs. Very recently, Yordanov et al. presented a photo-activated fluorescence from core/shell quantum dots of CdSe/CdS incorporated in a poly(butylmethacrylate) matrix (110). Since the toxicity of Cd, Se, As, or Pb-containing materials may lower their applicability in commercial devices, other PL semiconductor nanocrystals, such as doped ZnS, were also used as inorganic nano-fillers for PL PINCs (111).

A general concern for PL PINCs is that the PL of semiconductor nanocrystals can be destroyed when incorporated into polymer matrix. Therefore, core-shell structures of PL semiconductor nanocrystals are always employed and surface modification/engineering of semiconductor nanocrystals is usually needed to protect the PL of semiconductor nanocrystals.

Extreme refractive index (RI)

Compared to inorganic solids, optical applications of polymers are often limited due to the relatively narrow range of the RI. The RI values of most commercial polymers are typically located between 1.3 and 1.7, while inorganic materials can possess RI far below 1 (e.g. Au) or above 3 (e.g. PbS). Thus, the introduction of inorganic nanoparticles into a polymer matrix can result in polymeric nanocomposites with extreme RI, which finds potential applications in lenses, optical filters, reflectors, optical waveguides, optical adhesives, solar cells, or antireflection films (1). For high RI PINCs, PbS was the mostly studied inorganic additive (112–114). Other inorganic nano-fillers to enhanced RI included silicon (115), ZnS (116), and iron sulfides (117). Ultrahigh RI of 2.5–3.2 was achieved on PINCs with additives of PbS, silicon, or iron sulfides. With a ZnS content of 50 wt%, the RI of ZnS/poly(N,N-dimethylacrylamide) nanocomposite was increased from 1.54 to 1.63 (116). Analogously, the ultralow RI of 1 was also obtained on PINCs by incorporating Au nanoparticles into gelatin (118), which is the lowest RI known so far for PINCs. The content of Au was as high as 90 wt%.

From most studies, the RI of nanocomposites depends linearly on the content of the nano-fillers (both increase and decrease) (113, 115, 117, 118). Notably, when quantum confinement has to be considered for semiconductor nanocrystals as additives for PINCs, RI also becomes size-dependent besides other optical properties such as color and absorption coefficient. For example,

Kyprianidou-Leodidou et al. (119) reported a distinct decrease of RI with PbS nanoparticles below 25 nm compared to bulk PbS.

Dichroism

Dichroism was found on PINCs comprised of natural polymer (e.g. plant and animal fibrils) and metal particles (e.g. Ag and Au) more than 100 years ago (11). When metal particles are uniaxially oriented in the polymer matrix, linearly polarized light interacts differently when the angle between the polarization plane of the light and the long axis of the particle arrangement (φ) is 0 and 90°, respectively (12). As a result, different colors arise at parallel and perpendicular orientation. For example, the PINC comprised of Au and spruce wood fibers turned its color from red to blue green when φ was changed from 0 to 90°. Recently, dichroic PINCs were also produced by the solid-state drawing of isotropic nanocomposites (120–122) or on stretching of molten nanocomposite films in a controlled uniform extensional flow (123). PVA, polyethylene and poly(ethylene-co-vinyl alcohol) were employed as the polymer matrix and Au or Ag particles as inorganic additives. The dichroic colors depended on the type of metals as well as the particle diameters. The dichroism was also reflected by UV-Vis spectra recorded with polarized light. Anisotropic structures, such as Au nanorods, were also embedded into the polymer matrix (124, 125), since they have enormous absorption coefficients, tunable peak positions, and high photostability. As shown in Fig. 6, different colors of PVA composite films containing oriented Au nanorods have been observed, when placed parallel and perpendicular to the polarization direction induced by a polarizer placed on top (125). Uniaxially oriented Au nanorods was obtained by drawing/stretching the nanocomposite films and hence, dichroic PINCs were achieved. Dichroic

PINCs are promising materials as optical filters, making them potential candidates for liquid crystal displays.

Magnetic properties and applications of PINCS

Electromagnetic (EM) wave absorption

EM wave absorption materials have attracted much attention due to the expanded EM interference problems. The major application for this area is in the military for stealthy aircraft, boats, war ships, and so on. Currently the EM absorbers are being studied for taking more advantage of their properties such as lightweight, wide absorption frequency, high thermal stability, and antioxidation. The suggested properties could be tuned by changing the filler materials such as inorganic magnetic particles, metal nanoparticles and whiskers or nanotubes. Moreover, the final composition, concentration, and crystallinity of the filler also have strong influence on their EM wave absorption properties. The complicated multilayer structures of the layer by layer process could enhance their properties. Several attempts have been done with CNTs, iron and zinc oxide, and so on. However, the attenuation mechanism of those materials is mainly based on either dielectric loss or magnetic loss (126). The EM wave absorbing characteristics, such as matching frequency, matching thickness, and bandwidth need to be considered for designing the proper absorber. The absorption or dispersion of the EM energy in the medium (i.e. between the EM wave and a protected target by the use of radar absorbing materials to cover the metallic surface) is one of the methods of reducing the radar signature of the targets. Since the complex ε of the ferrite absorber show rather constant values in the GHz ranges, the EM wave absorbing characteristics strongly depend on the resonance phenomena of the ferrite filler. A proper combination of complex permeability and permittivity is
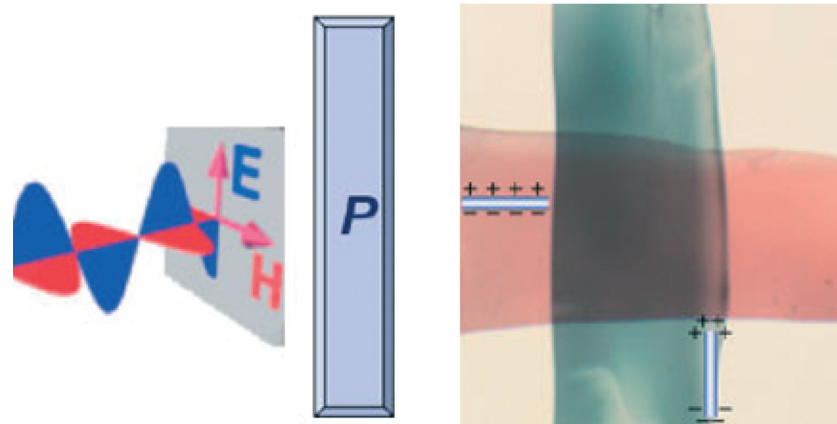

Fig. 6. Photograph of PVA films containing Au nanorods aligned parallel (blue film) and perpendicular (red film) to the electric field of polarized incoming light as schematically shown on the left. The bar labeled P represents a polarizer. (Adapted from Ref. (125). Reproduced with permission from Wiley-VCH Verlag GmbH & Co. KGaA.)

necessary to fabricate the zero-reflection EM wave absorber with an impedance matching. An increase of dielectric permittivity and the development of an impedance matching are important in a ferrite–polymer composite by adding conducting materials.

Chen et al. (126) reported core/shell structure of porous Fe_3O_4/Fe/SiO_2 nanorods with a length of 80 nm and 1.0 μm for EM wave absorption applications. The EM data show that the bandwidth with the reflection loss below −10 dB is up to 6.96 GHz, with 2 mm in thickness of the absorbers. Wei et al. (127) reported magnetic hollow spheres of low density prepared by plating Fe_3O_4 films on hollow glass spheres using ferrite plating. As shown in Fig. 7, the magnetic resonance frequency of sample B (composites with volume fraction 80%), was at about 13 GHz and it appeared three loss peaks in the calculated reflection loss curves; the bandwidth less than −10 dB was almost 4 GHz, which was just in the Ku-band frequencies (12–18 GHz) and a minimum reflection loss of −20 dB was obtained when the thickness was 2.6 mm; the microwave absorbing properties were mainly due to the magnetic loss. The results showed that the magnetic sphere composites were good and light microwave absorbers in the Ku-band frequencies. Ma et al. (128) reported the Fe/SiO_2 nanocomposite prepared by milling the mixture of Fe_2O_3 and Si powders for 40 hours in the stainless steel vial with stainless steel balls under an argon atmosphere. It shows that the broad resonance band in the 1–16 GHz range is due to the coexistence of natural resonance and exchange resonance. The double resonance behavior may result from the different spin precessions in the Fe nanoparticles due to the different arrangements of surface and core spins in the Fe nanoparticles. From the work, a more broad resonance band could be achieved by Fe/SiO_2 nanocomposite because the starting materials are already well crystallized than other reported samples that were prepared by a coprecipitation method. The mechanical milling process

could achieve a better crystallite sample but it could induce an impurity phase from the mill and balls together with a longer process time. The EM wave absorption properties based on magnetic particles are mainly related to their crystallographic structure, particles size and dispersity in matrix. Even though nanoparticles with different morphologies with different EM properties could consolidate as a final sample, the monotonous structure will restrict being applied in complicated structures. Therefore, the polymeric matrix-based nano-composite, PINCs, are suggested to construct a more complicated structure with lightweight applications and versatile materials that not only combine the unique characteristics of the components, but also manifest mutualistic effects between the two species. However, inorganic or metallic nanoparticles and the organic polymer matrix are immiscible with a different gravity, thus it is difficult to produce the nanocomposite. To overcome those problems, there are several processes to modify the surface of the nanoparticles. Some of the most convenient and attractive routes to the fabrication of nanoparticles embedded in the polymer matrix involve *in-situ* generation of the nanoparticles through reduction or decomposition of appropriate precursors inside the monomer (10, 53).

Kim et al. (129) reported the EM wave absorption of $Ni_{0.5}Zn_{0.4}Cu_{0.1}Fe_2O_4$ ferrite nanoparticles embedded in the PMMA matrix. The polymeric nanocomposite was prepared with the $Ni_{0.5}Zn_{0.4}Cu_{0.1}Fe_2O_4$ ferrite nanoparticles, graphite, and PMMA by a mechanical mixing and molding process. Fig. 8 corresponds to the X-band measurements for the complex permittivity and complex permeability. Especially, when graphite with a high dielectric constant was added to the matrix, permittivity is also increased. Generally, the resonance under GHz frequency is both domain wall resonance and spin rotational resonance. However, the spin rotational resonance is more predominant than domain wall resonance
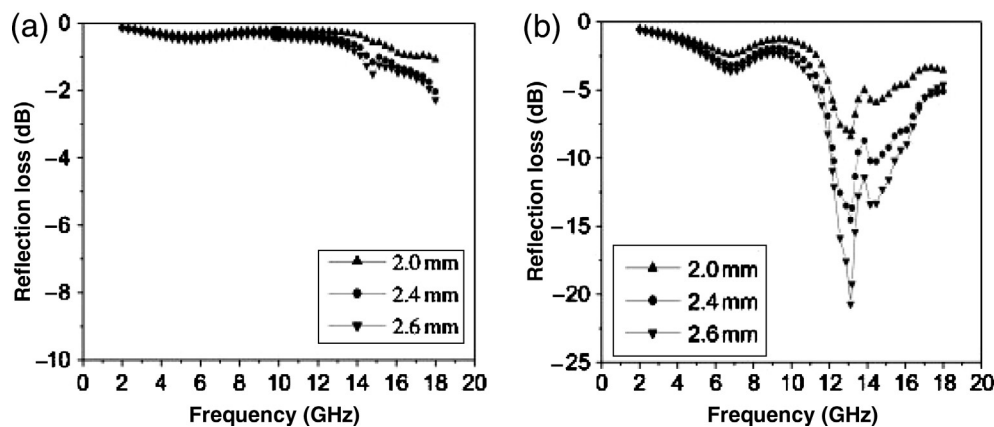

Fig. 7. Calculated reflection losses of samples with different magnetic spheres volume fractions: (a) 60% and (b) 80%, with different thicknesses. (Adapted from Ref. (127). Reproduced with permission from Elsevier B.V.)
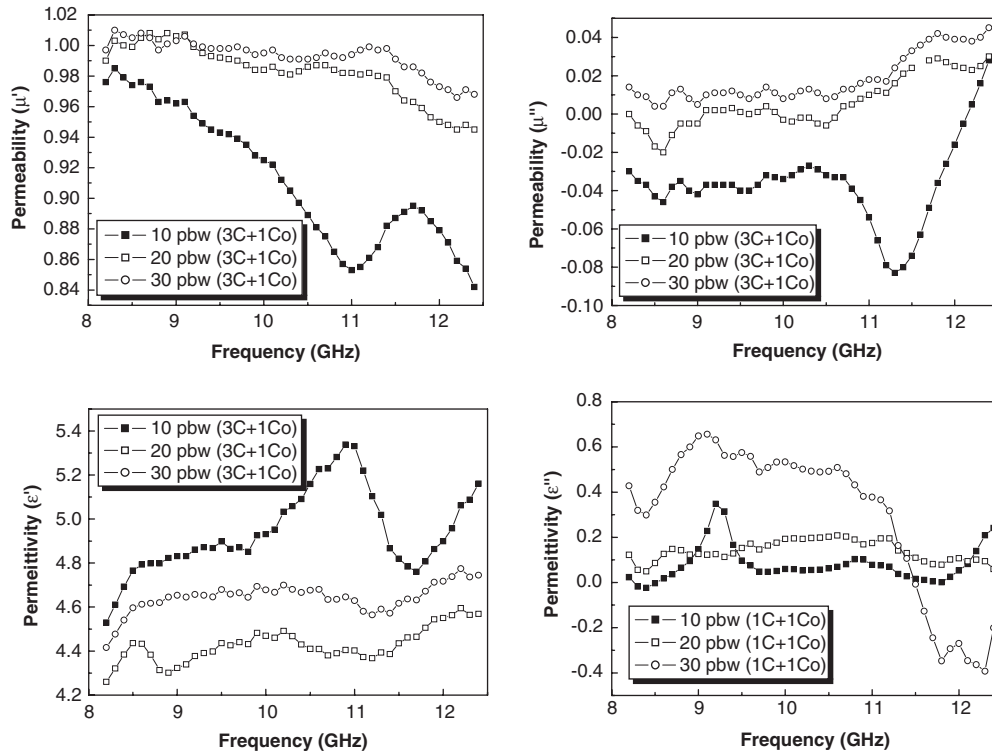
Fig. 8. Material constants spectra of composite specimens of 10, 20, and 30 pbw of 50% $Ni_{0.5}Zn_{0.4}Cu_{0.1}Fe_2O_4$ and 50% $CoFe_2O_4$ with a 5 pbw of graphite powder that was dispersed in PMMA with a thickness of 5 mm. μ′, μ′′, ε′, and ε′′. (Adapted from Ref. (129).)

when the ferrite particles as filler are sufficiently small to approach single domain characteristics. When the ferrite started to resonate, the complex permeability of 50 wt% $Ni_{0.5}Zn_{0.4}Cu_{0.1}Fe_2O_4$ (μ′) is drastically decreased and the μ′′ showed maximum peaks at a certain frequency. In this work, the μ′ value was increased as the amount of the filler was increased and the complex permeability of 50 wt% $CoFe_2O_4$ (μ′′) remained almost constant. Fig. 8 clearly shows that the permittivity is decreased with increasing concentration of the filler in polymeric matrix.

The normalized input impedance of a microwave-absorbing layer backed by a reflector at the absorber surface (Z_{in}) is given by (130):

$$Z_{in} = (\mu_r/\varepsilon_r)^{1/2} \tan h[j2\pi/c(\mu_r\varepsilon_r)^{1/2}fd], \quad (4)$$

where μ_r is the complex relative permeability of the materials; ε_r is the complex relative permittivity of the materials; is the frequency of the microwave in free space, and d is the thickness of an absorber, since the reflection loss is a function of Z_{in}, which is expressed as a reflection loss (R):

$$R = [db] = 20 \log(|(Z_{in} - 1)/(Z_{in} + 1)|). \quad (5)$$

From Equation 4, a proper combination of complex permeability (μ), permittivity (ε), thickness of absorber (d), and wavelength (λ) is necessary to fabricate the zero-reflection microwave absorber with an impedance matching (131). By an impedance matching solution map, the thickness and proper absorption frequency can be determined for zero-reflection. The permittivity is also affected by the filler concentration in the polymeric matrix. This difference is significant at P-band (Fig. 9).

The complex permittivity depends on the resistivity of the composite and can give qualitative information about the morphology of the phase. When the filler is conductive, the complex permittivity of 50 wt% $CoFe_2O_4$ (ε′′) can show if there is an electrical percolation. In this case, ferrites are very low conductive materials, but it can be seen that percolation might be achieved with 50 wt% $Ni_{0.5}Zn_{0.4}Cu_{0.1}Fe_2O_4$ by increasing the complex permittivity value with the filler concentration. Fig. 9 shows the absorption for the samples containing 20 and 70 wt% $Ni_{0.5}Zn_{0.4}Cu_{0.1}Fe_2O_4$ with a sample thickness of 10 mm. The nanocomposite with 20 wt% $Ni_{0.5}Zn_{0.4}Cu_{0.1}Fe_2O_4$ shows strong EM wave absorption at 15.2 GHz a magnitude of 25.4 dB whereas the composite with 70 wt% $Ni_{0.5}Zn_{0.4}Cu_{0.1}Fe_2O_4$ does not show absorption in these frequency ranges. Other work also reported on EM properties of PANI-based hexaferrite composites of PANI/$BaFe_{12}O_{19}$ composite by a facile *in-situ polymerization* of aniline in the presence of $BaFe_{12}O_{19}$ nanoparticles (132).
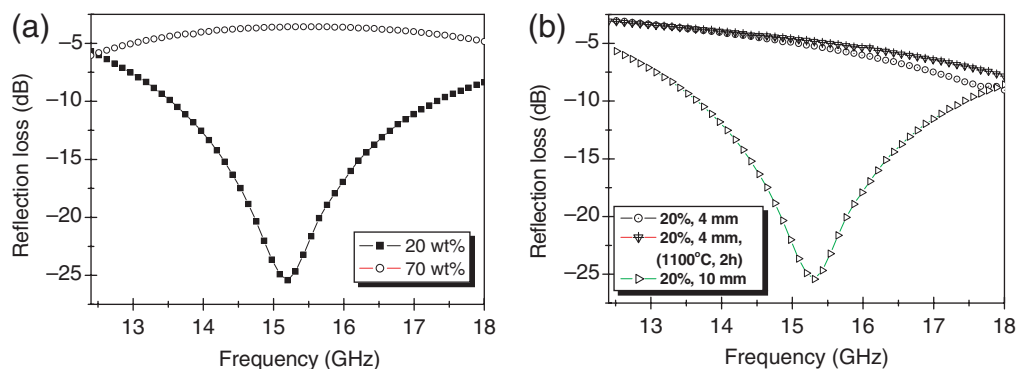
Fig. 9. (a) Microwave absorption for 20 and 70 wt% $Ni_{0.5}Zn_{0.4}Cu_{0.1}Fe_2O_4$ nanocomposites with a thickness of 10 mm. (b) 20 wt% $Ni_{0.5}Zn_{0.4}Cu_{0.1}Fe_2O_4$ nanocomposites with different samples thickness and prepared without and with heat treatment at 1,100°C for 2 hours. (Adapted from Ref. (129).)

Electromagnetic interference (EMI) shielding

EMI, a specific kind of environmental pollution, is drawing more attention recently, because of the explosive growth in the utilization of electrical and electronic devices in industrial, commercial, and military applications (133). Unfortunately, the EM wave emissions from one device could interfere with other devices, causing potential problems including a chronic disease such as damaging brain cells and DNA. To overcome these problematic EMI shielding problems, EM wave absorbers with the capability of shielding unwanted EM fields are required by using proper fillers (inorganic/metallic) and conducting polymer matrix. The EM wave absorption materials in section *EM wave absorption* can be used to minimize EM reflections from metal plates. Generally, a polymer-based nanocomposite containing electrically conductive fillers are widely used for the EMI

shielding of electronics (134). Yang and Gupta (135) reported a nanotube-PS foam composite as an effective EMI shielding materials. Single-absorber systems cannot realize low reflection loss in the wide band range. In contrast, Guo et al. (136) compared the reflection loss of Fe-O based samples composed of single-layer core-shell composite silica coated hematite ($FO@SiO_2$) and multi-layer structures (with mesoporous silica deposited on the surface of $FO@SiO_2$) at a frequency range of 2–18 GHz in Fig. 10, after mesoporous silica deposition on the surface of $FO@SiO_2$, the maximum RI value was increased to -4.95 dB at 15.80 GHz. The results clearly indicating that microwave absorbers with multilayer structures usually exhibit a wider absorption spectrum range and lower reflection loss compared to single-layer absorbers (136). The conductive polymer plays an important role in technologies such as stealth,
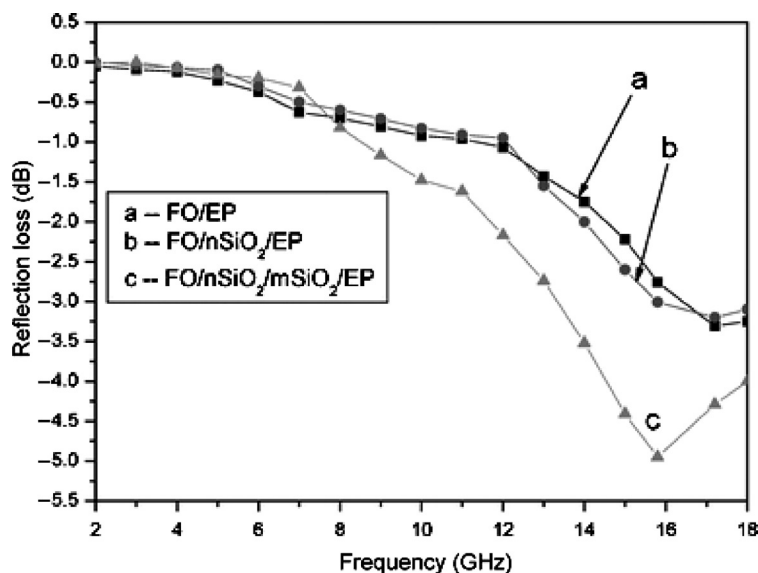

Fig. 10. Frequency dependence of the reflection loss of the iron oxide (FO)-based samples with component and structure variation: (a) FO/epoxide resin (EP); (b) $FO@SiO_2@/EP$; and (c) $FO@SiO_2@$mesoporous silica ($mSiO_2$)/EP. (Adapted from Ref. (136). Reproduced with permission from The Royal Society of Chemistry.)

electrostatic charge dissipation, and EMI shielding. Among conducting polymers, PANI is the most versatile because of their desirable properties, such as thermal and chemical stability, low specific mass, controllable conductivity, and high conductivity at microwave frequencies (137). Other interesting nanocomposites are bilayered thin films of ferrimagnetic $BaFe_{12}O_{19}$ and ferroelectric $Ba_{0.5}Sr_{0.5}TiO_3$ (138) and Fe-doped ZnO coated barium ferrite composite particles (139).

Summary and future outlook

Optical properties/applications of PINCs, including *light absorption (UV and color)*, *photoluminescence*, *extreme refractive index*, *dichroism*, and so on have made PINCs an important group of functional materials for centuries. Recently, the magnetic properties/applications of PINCs, including *EM wave absorption* and *EMI Shielding* attracted a lot of attention as well. Nevertheless, in spite of the significant advance in the past decades, the area of PINCs is not exhausted by far (140). Only a limited number of inorganic nano-fillers have been considered for nanocomposites. It is expected that the use of a new functional inorganic nano-filler will lead to PINCs with the unique combination of material properties. By careful selection of synthetic techniques and understanding/ exploiting the unique physics of the polymeric nanocomposites in such materials, the novel, functional PINCs can be designed and fabricated for new interesting applications such as *optoelectronic* and *magneto-optic* applications. For example, by selecting the transparent polymer as a bulk matrix and very little amounts of nano-fillers, optical transparencies, and homogeneous PINCs can be designed and synthesized by an *in-situ polymerization* technique; depending on the selection of inorganic nano-fillers such as specially band-gap tailored QDs or superparamagnetic nanoparticles, PINCs can be utilized as a gain medium for lasers (optoelectronic) or an active component in optical isolators (magneto-optic) (53). Other optoelectronic applications such as in solar cells and light-emitting diodes (LED) can also be explored based on PINCs incorporation of QDs in organic semiconductor polymers/conducting polymers (141–144). These new bifunctional applications, optoelectronic and magneto-optic, are believed to be the promising new lines of exploration of PINCs.

Acknowledgements

Conflict of interest and funding

There is no conflict of interest in the present study for any of the authors.

References

1. Althues H, Henle J, Kaskel S. Functional inorganic nanofillers for transparent polymers. Chem Soc Rev 2007; 36: 1454–65.
2. Ramanathan T, Stankovich S, Dikin DA, Liu H, Shen H, Nguyen ST, et al. Graphitic nanofillers in PMMA nanocomposites: an investigation of particle size and dispersion and their influence on nanocomposite properties. J Polymer Sci B Polymer Phys 2007; 45: 2097–112.
3. Vaisman L, Wachtel E, Wagner HD, Marom G. Polymer– nanoinclusion interactions in carbon nanotube based poly-acrylonitrile extruded and electrospun fibers. Polymer 2007; 48: 6843–54.
4. Okada A, Usuki A. Twenty years of polymer–clay nanocomposites. Macromol Mater Eng 2006; 291: 1449–76.
5. Okada A, Usuki A. The chemistry of polymer–clay hybrids. Mater Sci Eng C 1995; 3: 109–15.
6. Schottner G. Hybrid sol–gel-derived polymers: applications of multifunctional materials. Chem Mater 2001; 13: 3422–35.
7. Arafa IM, Fares MM, Barham AS. Sol–gel preparation and properties of interpenetrating, encapsulating and blend silica-based urea–formaldehyde hybrid composite materials. Eur Polymer J 2004; 40: 1477–87.
8. Zhang J, Luo S, Gui L. Poly(methyl methacrylate)–titania hybrid materials by sol–gel processing. J Mater Sci 1997; 32: 1469–72.
9. Yuwono AH, Liu B, Xue J, Wang J, Elim HI, Ji W, et al. Controlling the crystallinity and nonlinear optical properties of transparent TiO_2–PMMA nanohybrids. J Mater Chem 2004; 14: 2978–87.
10. Li S, Toprak MS, Jo YS, Dobson J, Kim DK, Muhammed M. Bulk synthesis of transparent and homogeneous polymeric hybrid materials with ZnO quantum dots and PMMA. Adv Mater 2007; 19: 4347–52.
11. Caseri W. Inorganic nanoparticles as optically effective additives for polymers. Chem Eng Comm 2009; 196: 549–72.
12. Caseri W. Nanocomposites of polymers and metals or semiconductors: historical background and optical properties. Macromol Rapid Comm 2000; 21: 705–22.
13. Lüdersdorff FW. Verh. Verein. Beförderung Gewerbefleiss. Preussen 1833; 12: 224.
14. Neri A. The art of glass, wherein are shown the wayes to make and colour glass, pastes, enamels, lakes and other curiosities. London: A.W.; 1662 (facsimile edition by UMI Books on Demand, Ann Arbor, MI, 2002).
15. Faraday M. The bakerian lecture: experimental relations of gold (and other metals) to light. Phil Trans R Soc Lond 1857; 147: 145–81.
16. Njugun J, Peilichowski K. Polymer nanocomposites for aerospace applications: fabrication. Adv Eng Mater 2004; 6: 193–210.
17. Hopf H, Gerasimov GN, Chavalun SN, Rozenberg VI, Popova EL, Nikolaevam EV, et al. Metal-containing poly (p-xylylene) films by CVD: poly (p-xylylene) with germanium crystals. Chem Vap Deposition 1997; 3: 197–200.
18. Macanas J, Parrondo J, Munoz M, Alegret S, Mijangos F, Muraviev DN. Preparation and characterisation of metal-polymer nanocomposite membranes for electrochemical applications. Phys Stat Sol (a) 2007; 204: 1699–705.

19. Ahmad S, Agnihotry SA, Ahmad S. Nanocomposite polymer electrolytes by in situ polymerization of methyl methacrylate: for electrochemical applications. J Appl Polymer Sci 2008; 107: 3042–8.

20. Grossiord N, Loos J, van Laake L, Maugey M, Zakri C, Koning CE, et al. High-conductivity polymer nanocomposites obtained by tailoring the characteristics of carbon nanotube fillers. Adv Func Mater 2008; 18: 3226–34.

21. Agarwal S, Khan MMK, Gupta RK. Thermal conductivity of polymer nanocomposites made with carbon nanofibers. Polymer Eng Sci 2008; 48: 2474–81.

22. Lévy R, Shaheen U, Cesbron Y, Sée V. Gold nanoparticles delivery in mammalian live cells: a critical review. Nano Reviews 2010; 1: 4889.

23. Lin MM, Kim HH, Kim H, Muhammed M, Kim DK. Iron oxide-based nanomagnets in nanomedicine: fabrication and applications. Nano Rev 2010; 1: 4883.

24. Owens DE, Eby JK, Jian Y, Peppas NA. Temperature-responsive polymer-gold nanocomposites as intelligent therapeutic systems. J Biomed Mater Res 2009; 3: 692–5.

25. Kim JH, Park K, Nam HY, Lee S, Kim K, Kwon IC. Polymers for bioimaging. Progr Polym Sci 2007; 32: 1031–53.

26. Wilson JL, Poddar P, Frey NA, Srikanth H, Mohomed K, Harmon JP, et al. Synthesis and magnetic properties of polymer nanocomposites with embedded iron nanoparticles. J Appl Phys 2004; 95: 1439–43.

27. Burke NAD, Stöver DH, Dawson FP. Magnetic nanocomposites: preparation and characterization of polymer-coated iron nanoparticles. Chem Mater 2002; 14: 4752–61.

28. Fang J, Tung LD, Stokes KL, He J, Caruntu D, Zhou WL, et al. Synthesis and magnetic properties of CoPt-poly(methylmethacrylate) nanostructured composite material. J Appl Phys 2002; 91: 8816–8.

29. Gangopadhyay R, De A. Polypyrrole-ferric oxide conducting nanocomposites I: synthesis and characterization. Eur Polymer J 1999; 35: 1985–92.

30. Gass J, Poddar P, Almand J, Srinath S, Srikanth H. Superparamagnetic polymer nanocomposites with uniform Fe_3O_4 nanoparticle dispersions. Adv Funct Mater 2006; 16: 71–5.

31. Prabhakaran T, Hemalatha J. Synthesis and characterization of magnetoelectric polymer nanocomposites. J Polymer Sci B Polymer Phys 2008; 46: 2418–22.

32. Balazs AC, Emrick T, Russell TP. Nanoparticle polymer composites: where two small worlds meet. Science 2006; 314: 1107–10.

33. Chen B, Evans JRG. Preferential intercalation in polymer-clay nanocomposites. J Phys Chem B 2004; 108: 14986–90.

34. Erdem N, Cireli AA, Erdogan UH. Flame retardancy behaviors and structural properties of polypropylene/nano-SiO_2 composite textile filaments. J Appl Polym Sci 2009; 111: 2085–91.

35. Hao C, Zhao Y, He A, Zhang X, Wang D, Ma Q, et al. Investigation on the melt spinning fibers of PP/organoclay nanocomposites prepared by in-situ polymerization. J Appl Polym Sci 2010; 116: 1384–91.

36. Ray SS, Yamada K, Okamoto M, Ueda K. Polylactide-layered silicate nanocomposite: a novel biodegradable material. Nano Lett 2002; 2: 1093–6.

37. Zhao H, Li RKY. A study on the photo-degradation of zinc oxide (ZnO) filled polypropylene nanocomposites. Polymer 2006; 47: 3207–17.

38. Sooklal K, Hanus LH, Ploehn HJ, Murphy CJ. A blue-emitting CdS/dendrimer nanocomposite. Adv Mater 1998; 10: 1083–7.

39. Chae DW, Kim BC. Characterization on polystyrene/zinc oxide nanocomposites prepared from solution mixing. Polym Adv Technol 2006; 16: 846–50.

40. Saravanamuttu K, Du XM, Najafi SI, Andrews MP. Photo-induced structural relaxation and densification in sol–gel-derived nanocomposite thin films: implications for integrated optics device fabrication. Can J Chem 1998; 76: 1717–29.

41. Pavlidou S, Papaspyrides CD. A review on polymer-layered silicate nanocomposites. Prog Polymer Sci 2008; 33: 1119–98.

42. Vaia RA, Ishii H, Giannelis EP. Synthesis and properties of two-dimensional nanostructures by direct intercalation of polymer melts in layered silicates. Chem Mater 1993; 5: 1694–6.

43. Mehrotra V, Giannelis EP. Conducting molecular multilayers: intercalation of conjugated polymers in layered media. Mater Res Soc Synp Proc 1990; 171: 39–44.

44. Vaia RA, Giannelis EP. Polymer melt intercalation in organically-modified layered silicates: model predictions and experiment. Macromolecules 1997; 30: 8000–9.

45. Lee DC, Jang LW. Preparation and characterization of PMMA–Clay hybrid composite by emulsion polymerization. J Appl Polym Sci 1996; 61: 1117–22.

46. Kim TH, Jang LW, Lee DC, Choi HJ, Jhon MS. Synthesis and rheology of intercalated polystyrene/Na+-montmorillonite nanocomposites. Macromol Rapid Commun 2002; 23: 191–5.

47. Dirix Y, Bastiaansen C, Caseri W, Smith P. Preparation, structure and properties of uniaxially oriented polyethylene–silver nanocomposites. J Mater Sci 1999; 34: 3859–66.

48. Dirix Y, Darribere C, Heffels W, Bastiaansen C, Caseri W, Smith P. Optically anisotropic polyethylene–gold nanocomposites. Appl Optics 1999; 38: 6581–6.

49. Veinot JGC, Galloro J, Pugliese L, Pestrin R. Surface functionalization of cadmium sulfide quantum confined nanoclusters. 5. Evidence of facile surface-core electronic communication in the photodecomposition mechanism of functionalized quantum dots. Chem Mater 1999; 11: 642–8.

50. Park J, An K, Hwang Y, Park JG, Noh HJ, Kim JY, et al. Ultra-large-scale syntheses of monodisperse nanocrystals. Nature Mater 2004; 3: 891–5.

51. Bourgeat-Lami EJ. Organic–inorganic nanostructured colloids. Nanosci Nanotechnol 2002; 2: 1–24.

52. Park J, Lee E, Hwang NM, Kang M, Kim SC, Hwang Y, et al. One-nanometer-scale size-controlled synthesis of monodisperse magnetic iron oxide nanoparticles. Angew Chem Int Ed 2005; 117: 2932–7.

53. Li S, Qin J, Fornara A, Toprak M, Muhammed M, Kim DK. Synthesis and magnetic properties of bulk transparent PMMA/Fe-oxide nanocomposites. Nanotechnology 2009; 20: 6–11.

54. Guo Z, Lei K, Li Y, Ng HW, Prikhodko S, Hahn HT. Fabrication and characterization of iron oxide nanoparticles reinforced vinyl-ester resin nanocomposites. Composites Sci Tech 2008; 68: 1513–20.

55. Avella M, Errico ME, Martelli S, Martuscelli E. Preparation methodologies of polymer matrix nanocomposites. Appl Organometal Chem 2001; 15: 435–9.

56. Avella M, Errico ME, Martuscelli E. Novel PMMA/$CaCO_3$ nanocomposites abrasion resistant prepared by an in situ polymerization process. Nano Lett 2001; 1: 213–7.

57. Sunkara HB, Jethmalani JM, Ford WT. Solidification of colloidal crystals of silica. Hybrid Org–Inorg Composites 1995; 14: 181–91.

58. Kickelbick G. Concepts for the incorporation of inorganic building blocks into organic polymers on a nanoscale. Prog Polym Sci 2003; 28: 83–114.

59. Mao Y, Fung BM. Formation and characterization of anchored polymer coatings on alumina. Chem Mater 1998; 10: 509–17.

60. Lu C, Cheng Y, Liu Y, Liu F, Yang B. A facile route to ZnS-polymer nanocomposite optical materials with high nanophase

content via ray irradiation initiated bulk polymerization. Adv Mater 2006; 18: 1188–92.

61. Althues HP, Philipp SF, Kaskel S. Integration of zinc oxide nanoparticles into transparent poly(butanediolmonoacrylate) via photopolymerisation. J Nanosci Nanotechnol 2006; 6: 409–13.

62. Wang JY, Chen W, Liu AH, Lu G, Zhang G, Zhang JH, et al. Controlled fabrication of cross-linked nanoparticles/polymer composite thin films through the combined use of surface-initiated atom transfer radical polymerization and gas/solid reaction. J Am Chem Soc 2002; 124: 13358–9.

63. Fu X, Qutubuddin S. Polymer–clay nanocomposites: exfoliation of organophilic montmorillonite nanolayers in polystyrene. Polymer 2001; 42: 807–13.

64. Wu MH, Lu N, Lei L, Qi DM, Lin HM. Electrostatic absorption of azo initiator onto TiO_2 particles and *in situ* anchoring polymerization of butyl acrylate from modified TiO_2. Acta Polym Sin 2009; 5: 445–50.

65. Podsiadlo P, Kaushik AK, Arruda EM, Waas AM, Shim BS, Xu J, et al. Ultrastrong and stiff layered polymer nanocomposites. Science 2007; 318: 80–3.

66. Sarkar MD, Deb P. Synthesis and characterization of hybrid nanocomposites comprising poly(vinyl alcohol) and colloidal silica. Adv Polym Tech 2008; 27: 152–62.

67. Wang ZG, Zu XT, Xiang X, Lian J, Wang LM. Preparation and characterization of polymer/inorganic nanoparticle composites through electron irradiation. J Mater Sci 2006; 41: 1973–8.

68. Rong MZ, Zhang MQ, Zheng YX, Zeng HM, Walter R, Friedrich K. Irradiation graft polymerization of nano-inorganic particles: an effective means to design polymer based nanocomposites. J Mater Sci Lett 2000; 19: 1159–61.

69. Ginzburg VV, Balazs AC. Calculating phase diagrams for nanocomposites: the effect of adding end-functionalized chains to polymer/clay mixtures. Adv Mater 2000; 12: 1805–9.

70. Zhou XD, Gu HC. Synthesis of PMMA–ceramics nanocomposites by spray process. J Mater Sci Lett 2002; 21: 577–80.

71. Hench LL, West JK. The sol–gel process. Chem Rev 1990; 90: 33–72.

72. Wan M, Li J. Synthesis and electrical–magnetic properties of polyaniline composites. J Polym Sci Pol Chem 1998; 36: 2799–805.

73. Landry CJT, Coltrain BK, Landry MR, Fitzgerald JJ, Long VK. Poly(vinyl acetate)/silica-filled materials: material properties of in situ vs fumed silica particles. Macromolecules 1993; 26: 3702–12.

74. Silveira KF, Yoshida IV, Nunes SP. Phase-separation in PMMA silica sol–gel systems. Polymer 1995; 36: 1425–34.

75. Nakane K, Yamashita T, Iwakura K, Suzuki F. Properties and structure of poly(vinyl alcohol)/silica composites. J Appl Polymer Sci 1999; 74: 133–8.

76. Stefanithis ID, Mauritz KA. Microstructural evolution of a silicon oxide phase in a perfluorosulfonic acid ionomer by an in situ sol–gel reaction. 3. Thermal analysis studies. Macromolecules 1990; 23: 2397–402.

77. Deng Q, Moore RB, Mauritz KA. Novel nafion/ORMOSIL hybrids via in situ sol-gel reactions. 1. Probe of ORMOSIL phase nanostructures by infrared spectroscopy. Chem Mater 1995; 7: 2259–68.

78. Wen J, Wilkes GL. Organic/inorganic hybrid network materials by the sol–gel approach. Chem Mater 1996; 8: 1667–81.

79. Liu X, Peng Y, Ji S. A new method to prepare organic-inorganic hybrid membranes. Desalination 2008; 221: 376–82.

80. López-Quintela MA. Synthesis of nanomaterials in microemulsions: formation mechanisms and growth control. Curr Opin Colloid In 2003; 8: 137–44.

81. Uskokovic V, Drofenik M. Synthesis of materials within reverse micelles. Surf Rev Lett 2005; 12: 239–77.

82. Yan F, Texter J. Capturing nanoscopic length scales and structures by polymerization in microemulsions. Soft Matt 2006; 2: 109–18.

83. Asim N, Radiman S, Yarmo MA. Preparation and characterization of core-shell polyaniline/V_2O_5 nanocomposite via microemulsion method. Mater Lett 2008; 62: 1044–7.

84. Palkovits R, Althues H, Rumplecker A, Tesche B, Dreier A, Holle U, et al. Polymerization of w/o microemulsions for the preparation of transparent SiO_2/PMMA nanocomposites. Langmuir 2005; 21: 6048–53.

85. Ni Y, Ge X, Liu H, Zhang Z, Ye Q. In situ synthesis and characterization of spherical CdS/polyacrylamide nanocomposites by γ-irradiation in w/o microemulsion. Chem Lett 2001; 30: 924–5.

86. Ries G, Heller W, Puchta H, Sandermann H, Seidlitz HK, Hohn B. Elevated UV-B radiation reduces genome stability in plants. Nature 2000; 406: 98–101.

87. Dickerson RR, Kondragunta S, Stenchikov G, Civerolo KL, Doddridge BG, Holben BN. The impact of aerosols on solar ultraviolet radiation and photochemical smog. Science 1997; 278: 827–30.

88. Masui T, Yamamoto M, Sakata T, Mori H, Adachi G. Synthesis of BN-coated CeO_2 fine powder as a new UV blocking material. J Mater Chem 2000; 10: 353–7.

89. Zheng J, Siegel RW, Toney CG. Polymer crystalline structure and morphology changes in nylon-6/ZnO nanocomposites. J Polym Sci Polym Phys 2003; 41: 1033–50.

90. Khrenov V, Klapper M, Koch M, Mullen K. Surface functionalized ZnO particles designed for the use in transparent nanocomposites. Macromol Chem Phys 2005; 206: 95–101.

91. Xiong M, Gu G, You B, Wu L. Preparation and characterization of poly(styrene butylacrylate) latex/nano-ZnO nanocomposites. J Appl Polym Sci 2003; 90: 1923–31.

92. Sun D, Miyatake N, Sue HJ. Transparent PMMA/ZnO nanocomposite films based on colloidal ZnO quantum dots. Nanotechnology 2007; 18: 215606–10.

93. Allen NS, Edge M, Ortega A, Sandoval G, Liauw CM, Verran J, et al. Degradation and stabilisation of polymers and coatings: nano versus pigmentary titania particles. Polym Degrad Stab 2004; 85: 927–46.

94. Hung CH, Whang WT. Effect of surface stabilization of nanoparticles on luminescent characteristics in ZnO/poly(hydroxyethyl methacrylate) nanohybrid films. J Mater Sci 2005; 15: 267–74.

95. Faubl H, Quinn MH. Spectra of UV-absorbing contact lenses: relative performance. Int Contact Lens Clin 2000; 27: 65–74.

96. Brus LE. Electron–electron and electron–hole interactions in small semiconductor crystallites: the size dependence of the lowest excited electronic state. J Chem Phys 1984; 80: 4403–7.

97. Brus LE. Electronic wave functions in semiconductor clusters: experiments and theory. J Phys Chem 1986; 90: 2555–61.

98. Pesika NS, Stebe KJ, Searson PC. Determination of the particle size distribution of quantum nanocrystals from absorbance spectra. Adv Mater 2003; 15: 1289–91.

99. Meulenkamp EA. Synthesis and growth of ZnO nanoparticles. J Phys Chem B 1998; 102: 5566–72.

100. Heffels W, Friedrich J, Darribère C, Teisen J, Interewicz K, Bastiaansen C, et al. Polymers and metals: nanocomposites and complex salts with metallic chain structure. Recent Res Devel Macromol Res 1997; 2: 143–56.

101. Maxwell Garnett JC. Colours in metal glasses and in metallic films. Phil Trans R Soc Lond A 1904; 203: 385–420.

102. Maxwell Garnett JC. Colours in metal glasses, in metallic films, and in metallic solutions-II. Phil Trans R Soc Lond A 1906; 205: 237–88.

103. Chan WCW, Nie S. Quantum dot bioconjugates for ultra-sensitive nonisotopic detection. Science 1998; 281: 2016–8.

104. Lee J, Sundar VC, Heine JR, Bawendi MG, Jensen KF. Full color emission from II–VI semiconductor quantum dot-polymer composites. Adv Mater 2000; 12: 1102–5.

105. Erskine L, Emrick T, Alivisatos AP, Fréchet JMJ. Preparation of semiconductor nanocrystal–polystyrene hybrid materials. Polym Prep 2000; 41: 593–4.

106. Farmer SC, Patten TE. Photoluminescent polymer/quantum dot composite nanoparticles. Chem Mater 2001; 13: 3920–6.

107. Zhang H, Cui Z, Wang Y, Zhang K, Ji X, Lü C, et al. From water-soluble CdTe nanocrystals to fluorescent nanocrystal–polymer transparent composites using polymerizable surfactants. Adv Mater 2003; 15: 777–80.

108. Sun ZB, Dong XZ, Chen WQ, Nakanishi S, Duan XM, Kawata S. Multicolor polymer nanocomposites: in situ synthesis and fabrication of 3D microstructures. Adv Mater 2008; 20: 914–9.

109. Ventura MJ, Gu M. Engineering spontaneous emission in a quantum-dot-doped polymer nanocomposite with three-dimensional photonic crystals. Adv Mater 2008; 20: 1329–32.

110. Yordanov GG, Gicheva GD, Dushkin CD. Optical memory based on photo-activated fluorescence of core/shell quantum dots embedded in poly(butylmethacrylate). Mater Chem Phys 2009; 113: 507–10.

111. Althues H, Palkovits R, Rumplecker A, Simon P, Sigle W, Bredol M, et al. Synthesis and characterization of transparent luminescent ZnS:Mn/PMMA nanocomposites. Chem Mater 2006; 18: 1068–72.

112. Weibel M, Caseri W, Suter UW, Kiess H, Wehrli E. Preparation of polymer nanocomposites with "ultrahigh" refractive index. Polym Adv Technol 1991; 2: 75–80.

113. Zimmermann L, Weibel M, Caseri W, Suter UW. High refractive index films of polymer nanocomposites. J Mater Res 1993; 7: 1742–8.

114. Lü C, Guan C, Liu Y, Cheng Y, Yang B. PbS/polymer nanocomposite optical materials with high refractive index. Chem Mater 2005; 17: 2448–54.

115. Papadimitrakopoulos F, Wisniecki P, Bhagwagar DE. Mechanically attrited silicon for high refractive index nanocomposites. Chem Mater 1997; 9: 2928–33.

116. Lü C, Cheng Y, Liu Y, Liu F, Yang B. A facile route to ZnS–polymer nanocomposite optical materials with high nanophase content via γ-ray irradiation initiated bulk polymerization. Adv Mater 2006; 18: 1188–92.

117. Kyprianidou-Leodidou T, Margraf P, Caseri W, Suter UW, Walther P. Polymer sheets with a thin nanocomposite layer acting as a UV filter. Polym Adv Technol 1997; 8: 505–12.

118. Zimmermann L, Weibel M, Caseri W, Suter UW, Walter P. Polymer nanocomposites with "ultralow" refractive index. Polym Adv Technol 1993; 4: 1–7.

119. Kyprianidou-Leodidou T, Caseri W, Suter UW. Size variation of PbS particles in high-refractive-index nanocomposites. J Phys Chem 1994; 98: 8992–7.

120. Dirix Y, Bastiaansen C, Caseri W, Smith P. Oriented pearl-necklace arrays of metallic nanoparticles in polymers: a new route toward polarization-dependent color filters. Adv Mater 1999; 11: 223–7.

121. Heffels W, Bastiaansen C, Caseri W, Smith P. Oriented nanocomposites of ultrahigh-molecular-weight polyethylene and gold. Mol Cryst Liq Cryst 2000; 353: 191–201.

122. Pucci A, Bernabò M, Elvati P, Meza LI, Galembeck F, Alberto de Paula Leite C, et al. Photoinduced formation of gold nanoparticles into vinyl alcohol based polymers. J Mater Chem 2006; 16: 1058–66.

123. Schmid D, Handge UA, Gann JP, Yan M, Caseri W. Melt elongation of polymer nanocomposites: a method for the controlled production of dichroic films. Macromol Mater Eng 2008; 293: 471–8.

124. Murphy CJ, Orendorff CJ. Alignment of gold nanorods in polymer composites and on polymer surfaces. Adv Mater 2005; 17: 2173–7.

125. Pérez-Juste J, Rodríguez-González B, Mulvaney P, Liz-Marzán LM. Optical control and patterning of gold-nanorod-poly(vinylalcohol) nanocomposite films. Adv Funct Mater 2005; 15: 1065–71.

126. Chen YJ, Gao P, Zhu CL, Wang RX, Wang LJ, Cao MS, et al. Synthesis, magnetic and electromagnetic wave absorption properties of porous Fe_3O_4/Fe/SiO_2 core/shell nanorods. J Appl Phys 2009; 106: 054303–4.

127. Wei J, Liu J, Li S. Electromagnetic and microwave absorption properties of Fe_3O_4 magnetic films plated on hollow glass spheres. J Magn Magn Mater 2007; 312: 414–7.

128. Ma J, Li J, Ni X, Zhang X, Huang J. Microwave resonance in Fe/SiO_2 nanocomposite. Appl Phys Lett 2009; 95: 102505–3.

129. Kim DK, Toprak MS, Mikhaylova M, Jo YS, Savage S, Lee HB, et al. Polymeric nanocomposites of complex ferrite. Soli Stat Phenom 2003; 99–100: 165.

130. Giannakopoulou T, Kompotiatis L, Kontogeorgakos A, Kordas G. Microwave behavior of ferrites prepared via sol-gel method. J Magn Magn Mater 2002; 246: 360–5.

131. Musal HM, Hahn HT. Thin-layer electromagnetic absorber design. IEEE Trans Magn 1989; 25: 3851–3.

132. Jiang J, Ai LH, Qin DB, Liu H, Li LC. Preparation and characterization of electromagnetic functionalized polyaniline/$BaFe_{12}O_{19}$ composites. Synth Met 2009; 159: 695–9.

133. Ohlan A, Singh K, Dhawan SK. Shielding and dielectric properties of sulfonic acid-doped pi-conjugated polymer in 8.2–12.4 GHz frequency range. J Appl Polym Sci 2009; 115: 498–503.

134. Yang YL, Gupta MC, Dudley KL, Lawrence RW. Conductive carbon nanoriber-polymer foam structures. Adv Mater 2005; 17: 1999–2003.

135. Yang YL, Gupta MC. Novel carbon nanotube–polystyrene foam composites for electromagnetic interference shielding. Nano Lett 2005; 5: 2131–4.

136. Guo XH, Deng YH, Gu D, Che RC, Zhao DY. Synthesis and microwave absorption of uniform hematite nanoparticles and their core-shell mesoporous silica nanocomposites. J Mater Chem 2009; 19: 6706–12.

137. Phang SW, Tadokoro M, Watanabe J, Kuramoto N. Microwave absorption behaviors of polyaniline nanocomposites containing TiO_2 nanoparticles. Curr Appl Phys 2008; 8: 391–4.

138. Heindl R, Srikanth H, Witanachchi S, Mukherjee P, Weller T, Tatarenko AS, et al. Structure, magnetism, and tunable microwave properties of pulsed laser deposition grown barium ferrite/barium strontium titanate bilayer films. 10th Joint MMM/Intermag Conference, Baltimore, MD, 7–11 January 2007. Baltimore, MD: AIP; 2007, pp. 09M503–3.

139. Tang X, Hu KA. Preparation and electromagnetic wave absorption properties of Fe-doped zinc oxide coated barium ferrite composites. Mater Sci Eng B 2007; 139: 119–23.

140. Caseri WR. Nanocomposites of polymers and inorganic particles: preparation, structure and properties. Mater Sci Tech 2006; 22: 807–17.

141. Nozik AJ. Quantum dot solar cells. Phys E Low Dimensional Sys Nanostruct 2002; 14: 115–20.

142. Tomczak N, Janczewski D, Han M, Vancso GJ. Designer polymer-quantum dot architectures. Progr Polymer Sci 2009; 34: 393–430.

143. Lee CW, Chou CH, Huang JH, Hsu CS, Nguyen TP. Investigations of organic light emitting diodes with CdSe(ZnS) quantum dots. Mater Sci Eng B 2008; 147: 307–11.

144. Chung W, Park K, Yu HJ, Kim J, Chun B-H, Kim SH. White emission using mixtures of CdSe quantum dots and PMMA as a phosphor. Opt Mater 2010; 32: 515–21.

*Shanghua Li
KTH-FNM, Isafjordsgatan 22
SE-164 40 Kista, Sweden
Tel: +46 8 7908148
Fax: +46 8 7909072
Email: shanghua@kth.se